




Finding and Tracking a Phytoplankton Patch by a Long-Range Autonomous Underwater Vehicle

Yanwu Zhang , Senior Member, IEEE, Michael A. Godin, Brian Kieft, Ben-Yair Raanan, John P. Ryan , and Brett W. Hobson 

Abstract—Phytoplankton (microscopic algae) play an important role in marine ecology. Resulting from a combination of physical, chemical, and biological processes, the distribution of phytoplankton is patchy, particularly in coastal marine ecosystems. Patches of high chlorophyll represent areas where enhanced primary productivity and biogeochemical cycling can occur. The scientific goal is to place observations within these biological hotspots to enable more extensive characterization of the environment and plankton populations. Aerial or satellite remote sensing can detect optical signal originating from phytoplankton within a limited depth range only near the ocean surface, and application of remote sensing is limited by atmospheric clarity. To observe the development of patchy phytoplankton communities *in situ*, we need the ability to locate and track individual patches. In this article, we present a method for an autonomous underwater vehicle (AUV) to autonomously find and climb on a positive horizontal gradient of chlorophyll to locate and track a phytoplankton patch. In two experiments in 2021, a *Tethys*-class long-range AUV autonomously located and tracked phytoplankton patches in southern Monterey Bay, CA, USA. The experiments demonstrated effectiveness of the method and pointed to the need for increased onboard adaptiveness in autonomous patch finding and tracking.

Index Terms—Autonomous underwater vehicle (AUV), locate, track, phytoplankton patch.

I. INTRODUCTION

PHYTOPLANKTON photosynthesis accounts for approximately half of the global net primary production [1], [2], which supports marine life, supplies atmospheric oxygen, and sequesters anthropogenic carbon dioxide. Certain types of algal blooms produce toxins and cause harm to fisheries, aquaculture, marine mammals, and human health [3]. Owing to interacting physical, chemical, and biological processes, phytoplankton distributions are usually patchy [4], [5]. Patches of high chlorophyll represent areas where enhanced primary productivity and biogeochemical cycling can occur. The scientific goal is to

place observations within these biological hotspots to enable more extensive characterization of the environment and plankton populations. The patchiness, as well as the movement of plankton populations with ocean currents, introduces challenges to effective *in situ* observation and sampling.

To study the development of phytoplankton communities in a patch, we need the ability to locate and track individual patches. Satellite remote sensing has been used to track certain types of algal blooms [5] based on ocean-color measurement. However, satellite sensing is limited by cloud cover and low revisit frequency, both of which can lead to extended periods without data. In addition, satellites observe only the near-surface layer and, consequently, can miss the existence of subsurface phytoplankton patches. Therefore, complementary methods are needed for observation [6].

Autonomous underwater vehicles (AUVs) and autonomous surface vehicles were used for observing subsurface or surface chlorophyll patches by taking advantage of the vehicles' mobility, endurance, and onboard intelligence [7]–[9]. AUVs used olfactory-based search mechanisms to detect chemical plumes when the measurement exceeds a preset threshold and then make turns of a certain pattern to remain in or reacquire the plume [10], [11]. A gradient search algorithm was designed for locating hydrothermal vents or other oceanographic features signified by the global maximum or minimum in a field [12]. Algorithms were also designed using statistical modeling methods, e.g., mapping chlorophyll patches through a two-phase process: data collection and modeling in the first phase and adaptive mapping in the second phase [13].

The method presented in this article built upon the algorithm [7] in which the AUV maneuvers in repeated cycles of four different directions (e.g., in the order of west, south, east, and north) to figure out a direction of positive gradient and climb on that gradient. We present an improved algorithm, and the improvements include: 1) low-pass filtering of chlorophyll peaks on sequential yo-yo profiles for robust detection of the patch center and 2) the AUV ascends to the surface for global positioning system (GPS) fixes only at the start of the legs (rather than in the middle) to avoid disruption of the water reference frame calculation of the vehicle's distance to the maximum-chlorophyll location.

Tethys-class long-range AUVs (LRAUVs) are described in Section II. The algorithm is presented in Section III. A simulation test is demonstrated in Section IV. In February and April

Manuscript received June 6, 2021; revised October 2, 2021; accepted October 17, 2021. Date of publication December 20, 2021; date of current version April 13, 2022. This work was supported by the David and Lucile Packard Foundation and the National Oceanic and Atmospheric Administration under Grant NA19NOS4780181. (Corresponding author: Yanwu Zhang.)

Associate Editor: T. Maki.

Yanwu Zhang, Brian Kieft, Ben-Yair Raanan, John P. Ryan, and Brett W. Hobson are with the Monterey Bay Aquarium Research Institute, Moss Landing, CA 95039 USA (e-mail: yzhang@mbari.org; bkieft@mbari.org; byraanan@mbari.org; ryjo@mbari.org; hobson@mbari.org).

Michael A. Godin is with IntuAware, Northampton, MA 01062 USA (e-mail: mike@intuaware.com).

Digital Object Identifier 10.1109/JOE.2021.3122195

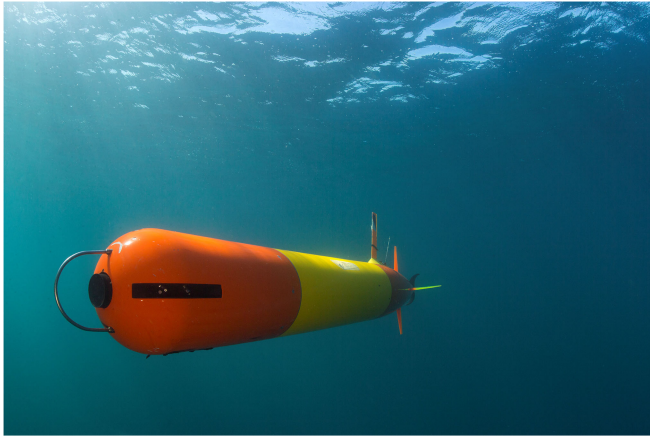


Fig. 1. *Tethys*-class LRAUV (photo courtesy of Kip Evans).

2021, a *Tethys*-class LRAUV located and tracked phytoplankton patches in southern Monterey Bay, as reported in Section V. The conclusion and future work are discussed in Section VI.

II. TETHYS-CLASS LRAUV

A *Tethys*-class LRAUV (see Fig. 1) is 2.3–3.2 m long (depending on the payload configuration) and has a diameter of 0.3 m at the midsection. It can run from 0.5 to 1 m/s using a propeller. Using a primary battery, the vehicle has demonstrated a range of 1800 km (three-week duration) at 1-m/s speed [14]. Long range is realized by minimizing propulsion power consumption through an innovative design of a low-drag body and a high-efficiency propulsion system [15]. In addition, the vehicle is equipped with a buoyancy engine and is capable of auto-ballasting to neutral buoyancy, which allows flight at a reduced angle of attack to decrease drag. Using the buoyancy engine, the vehicle is capable of drifting in a lower power state and controlling depth, while the thruster is powered off. An LRAUV thus combines mobility and speed properties typical to propelled vehicles and energy saving properties unique to buoyancy-driven vehicles. An LRAUV's science sensor suite (all in the nose section) includes SBE GPCTD temperature, conductivity, and depth sensors, a WET Labs BB2FL fluorescence/backscatter sensor (chlorophyll fluorescence excitation wavelength of 470 nm and emission wavelength of 695 nm), an Aanderaa 4831F dissolved oxygen sensor, and a LI-COR LI-192SA photosynthetically active radiation sensor.

The vehicle's underwater navigation is by dead reckoning aided by a Doppler velocity log (DVL). The DVL provides the earth-referenced velocity of the vehicle when the ocean bottom is within acoustic range. The vehicle's estimated speed is combined with measured heading and attitude and then accumulated to provide the estimated location. The vehicle periodically ascends to the surface for a GPS fix to correct the accumulated underwater navigation error [14].

The LRAUV software architecture uses state-configured layered control [16], which divides vehicle operation into a group of behaviors assigned with hierarchical levels of priority. The

vehicle runs a mission script that invokes appropriate AUV behaviors to achieve a specified goal [14], [17].

III. PATCH FINDING AND TRACKING ALGORITHM

The chlorophyll peak is both a biological indicator and the spatial signal that can be used to locate and track a phytoplankton patch. The algorithm comprises two parallel behaviors: chlorophyll peak detection in the vertical dimension and searching for the patch center in the horizontal dimension. The vertical-dimension peak-detection behavior extracts the chlorophyll peak on each yo-yo profile for use in the horizontal-dimension search behavior.

A. Vertical Dimension: Peak Detection on Each Yo-yo Profile

On each descent or ascent yo-yo profile, the AUV records the chlorophyll peak value on completion of that profile, as shown in Fig. 2(a). The vehicle keeps track of the start and end of each descent or ascent profile by detecting the attitude flip [18]. To remove spurious spikes due to sensor noise, the raw chlorophyll measurement goes through a five-point median filter (2-s duration corresponding to 0.6-m yo-yo depth change) followed by an 8-s moving-average window for low-pass filtering.

B. Horizontal Dimension: Cross-Pattern Search for Patch Center

For robust detection of the patch center, the per-yoyo chlorophyll peaks are low-pass filtered by averaging over a certain number of yo-yo profiles. This number is appropriately set for smoothing out small-scale variations, yet maintaining the overall gradient of the chlorophyll signal. The AUV searches in the four cardinal directions (north, west, east, and south) successively. For each direction, the vehicle yo-yoes outbound to look for the maximum chlorophyll and then yo-yoes inbound to return to the maximum-chlorophyll location. When that location is reached, the vehicle makes a 90° turn to search in the orthogonal direction. Due to ocean current, the “maximum-chlorophyll location” detected on the outbound leg will have been displaced by the time the vehicle returns to that location on the inbound leg, introducing a tracking error. Thus, there is an inherent tradeoff between the exploration time spent in search and the tracking error caused by the latency. The cross-shaped search pattern is selected over other patterns (e.g., a bowtie-like pattern) because its straight return distance is the shortest back to the “maximum-chlorophyll location.”

We first consider the case where the AUV starts the search near the patch center. Suppose the starting location is to the south of the center. The cross pattern comprises eight legs, which are numbered in Fig. 2(b) and explained as follows.

- ① *Northward leg*: When the AUV approaches the patch center, the per-yoyo peak chlorophyll value rises until reaching the maximum at the center. The vehicle records the maximum chlorophyll value (denoted by chl_{max}) and the corresponding location. When the vehicle leaves the center, the per-yoyo peak chlorophyll value drops. When the value drops below a preset percentage (denoted by

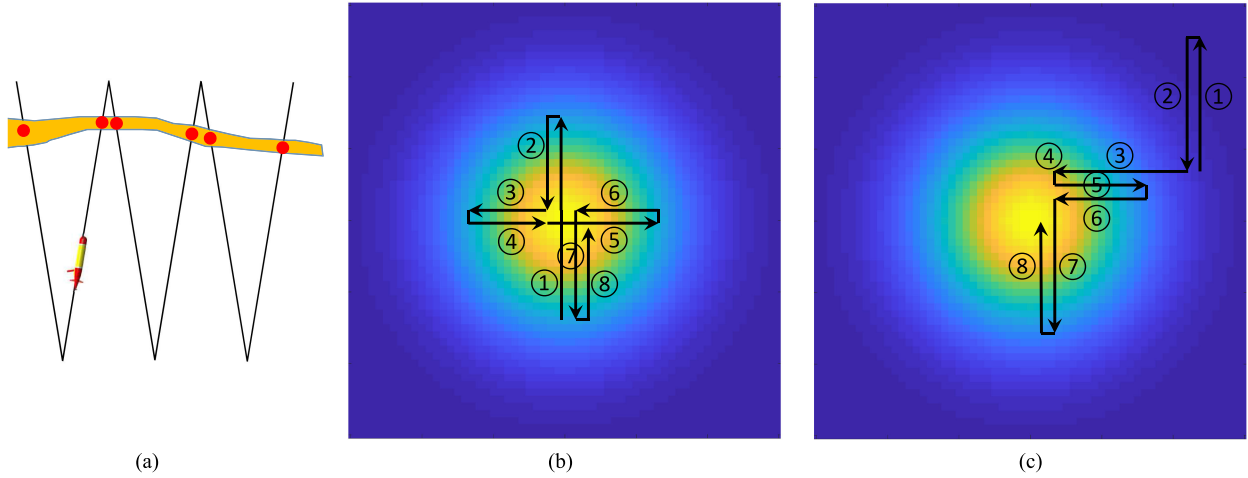


Fig. 2. Illustration of the patch finding and tracking algorithm. (a) Vertical dimension: detection of the chlorophyll peak on each yo-yo profile. (b) and (c) Horizontal dimension: one cycle of cross pattern when the search starts near the center (b) or far from the center (c). The short ticks between legs are imaginary insertions for clear graphical depiction of all legs.

Percentage_{Threshold}) of chl_{max} or the AUV has traveled the distance limit (denoted by $Dist_{LegMax}$), the vehicle determines to reverse course and calculates the distance to the recorded chl_{max} location (denoted by $Dist_{ToChlMax}$).

- ② *Southward leg*: The AUV travels $Dist_{ToChlMax}$ to return to the patch center. On this leg, the vehicle turns off the function of searching for chl_{max} .
- ③ *Westward leg*: Once returning to the patch center, the AUV makes a right turn to yo-yo westward. It turns on the search-for-maximum function to record chl_{max} and the corresponding location on this leg. When the vehicle leaves the patch center, the per-yoyo peak chlorophyll value drops. When the value drops below Percentage_{Threshold} · chl_{max} , the vehicle determines to reverse course and calculates $Dist_{ToChlMax}$.
- ④ *Eastward leg*: Same as leg 2 except for the direction.
- ⑤ *Continued eastward leg*: Same as leg 3 except that the AUV continues to yo-yo eastward after returning to the patch center.
- ⑥ *Westward leg*: Same as leg 2 except for the direction.
- ⑦ *Southward leg*: Same as leg 3 except that the AUV makes a left turn after returning to the patch center.
- ⑧ *Northward leg*: Same as leg 2 except for the direction.

The AUV repeats the cross pattern to track the patch center, while the center moves over time. Now, we consider the general case where the AUV starts far from the patch center. Suppose that the starting location is to the northeast of the center. The first eight legs of the search are numbered in Fig. 2(c) and explained as follows.

- ① *Northward leg*: The chlorophyll level is low on the entire northward leg, and the starting point has comparatively the highest level (i.e., chl_{max}). When the AUV yo-yoes northward, the chlorophyll level gradually drops. The chlorophyll level is still above Percentage_{Threshold} · chl_{max} when the vehicle has traveled the distance limit $Dist_{LegMax}$.

- ② *Southward leg*: The AUV returns to the chl_{max} location (i.e., the starting point of the preceding northward leg). On this leg, the vehicle turns off the function of searching for chl_{max} .
- ③ *Westward leg*: Once returning to the chl_{max} location, the AUV makes a right turn to yo-yo westward. It turns on the search-for-maximum function to record chl_{max} and the corresponding location on this leg. When the traveled distance reaches $Dist_{LegMax}$, the chlorophyll level also reaches the highest. To prepare for reversing course on the next leg, the vehicle now calculates $Dist_{ToChlMax}$, which is zero because the ending point is where the chlorophyll level is the highest on this leg.
- ④ *Eastward leg*: The AUV turns off the search-for-maximum function and reverses course to travel $Dist_{ToChlMax}$ to return to the chl_{max} location. Because $Dist_{ToChlMax}$ is zero, this leg is immediately completed, and the vehicle continues onto the next leg.
- ⑤ *Continued eastward leg*: The AUV turns on the search-for-maximum function and continues to yo-yo eastward. When the chlorophyll level drops below Percentage_{Threshold} · chl_{max} , the vehicle determines to reverse course and calculates $Dist_{ToChlMax}$.
- ⑥ *Westward leg*: The AUV turns off the search-for-maximum function and travels $Dist_{ToChlMax}$ to return to the chl_{max} location.
- ⑦ *Southward leg*: Once returning to the chl_{max} location, the AUV makes a left turn to yo-yo southward. It turns on the search-for-maximum function to record chl_{max} and the corresponding location on this leg. The chlorophyll level is still above Percentage_{Threshold} · chl_{max} when the vehicle has traveled $Dist_{LegMax}$. The vehicle now calculates $Dist_{ToChlMax}$ to prepare for the next leg.
- ⑧ *Northward leg*: The AUV returns to the chl_{max} location. On this leg, the vehicle turns off the search-for-maximum function.

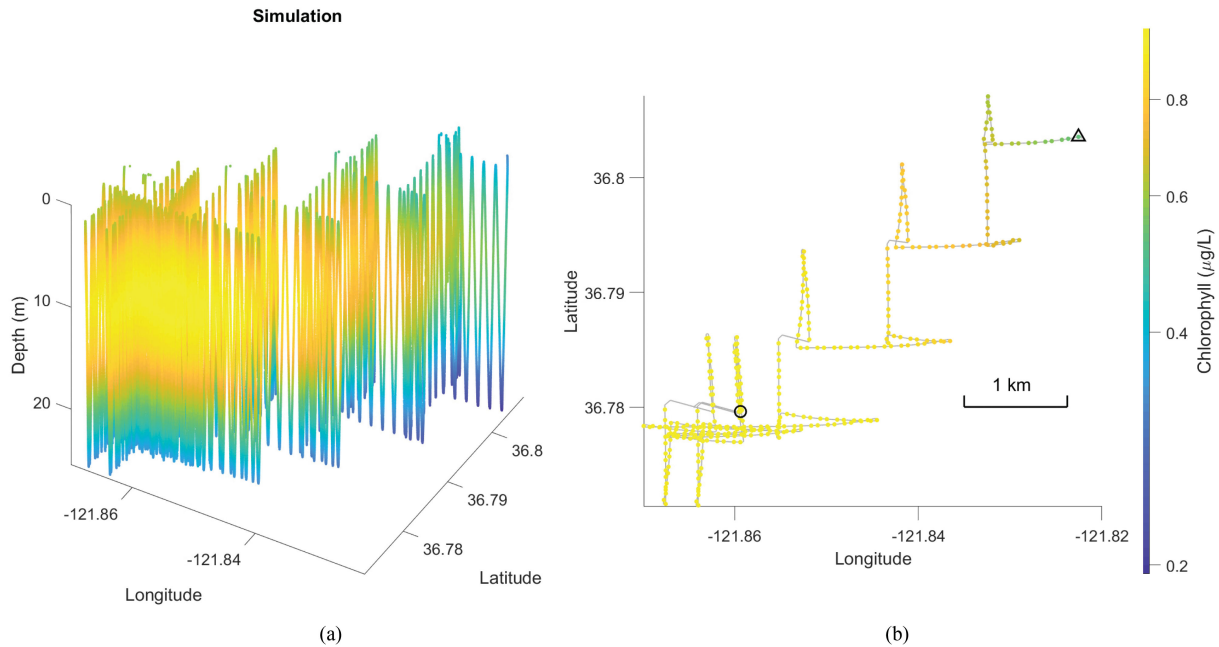


Fig. 3. Simulated search for the chlorophyll patch center. The AUV starts from the northeast and ends at the patch center. (a) Perspective view of chlorophyll levels on the yo-yo track. (b) The horizontal track is marked by the gray line; the chlorophyll peak values on successive yo-yo profiles are color coded. The start and end locations are marked by the triangle and the circle, respectively.

This way, the AUV climbs on a positive horizontal gradient of chlorophyll to approach the patch center. The succeeding legs for tracking the center will be similar to those illustrated in Fig. 2(b).

In field experiments, we set $\text{Dist}_{\text{LegMax}}$ to the typical scale of phytoplankton patches. If $\text{Dist}_{\text{LegMax}}$ is too long, the AUV may travel too far and, consequently, lose track of the targeted patch center; if it is too short, the vehicle may get trapped in a local chlorophyll maximum. We set $\text{Percentage}_{\text{Threshold}}$ based on how much the chlorophyll level drops over a distance of $\text{Dist}_{\text{LegMax}}$ when the AUV passes high-chlorophyll regions in reconnaissance missions (see Section V).

The vehicle periodically ascends to surface for GPS fixes and transmitting decimated data to shore via Iridium satellite. Every time the vehicle gets a GPS fix, it makes a correction to the underwater dead-reckoned navigation, leading to a “jump” of latitude and longitude readings. If the vehicle were to surface on a constant period, GPS fixes could occur in the middle of a leg. The resultant jump of latitude and longitude would disrupt the calculation of the distance between the turn-back point and the recorded chl_{max} location. To prevent this problem, the algorithm allows the vehicle to surface only at the start of a leg to ensure that the vehicle remains in the water reference frame for the full duration of the leg.

IV. SIMULATION TEST

We test the algorithm using a simulated chlorophyll field (see Fig. 3), which has a 3-D Gaussian distribution, centered at latitude 36.78° , longitude -121.86° , and 10-m depth. The AUV yo-yoes between 1.5- and 25-m depths on repeated cross patterns. The per-yoyo chlorophyll peaks are averaged over four

yo-yo profiles. $\text{Dist}_{\text{LegMax}}$ was set to 1 km; $\text{Percentage}_{\text{Threshold}}$ was set to 90%. The vehicle first climbs on a positive horizontal gradient of chlorophyll from the northeast to the center [as illustrated in Fig. 2(c)] and then stays at the center [as illustrated in Fig. 2(b)].

V. EXPERIMENTS

A. February 13 and 14, 2021

In an experiment from February 13 to 14, 2021, LRAUV *Pontus* was deployed in southern Monterey Bay to locate a phytoplankton patch. Measurements by a Visible Infrared Imaging Radiometer Suite instrument onboard the NOAA/NASA polar-orbiting satellite¹ show that sea surface chlorophyll levels were higher in near-shore shallow shelf waters on February 13 and 17 [see Fig. 4(a)]. The true-color image on February 17 taken by a Moderate Resolution Imaging Spectroradiometer instrument onboard the NASA Aqua satellite [see Fig. 4(b); using the SeaDAS software applied to data downloaded from <https://ladsweb.modaps.eosdis.nasa.gov/>] shows that most of the water in the bay was blue (indicating low chlorophyll levels), and greener water (indicating higher chlorophyll levels) was present in a ring around the inner bay and in a filament offshore.

Pontus' trajectory and the chlorophyll measurement are shown in Fig. 5. The vehicle started from a low-chlorophyll location offshore in the southwest. The vehicle yo-yoed from 1.5- to 15-m depths on repeated cross patterns. In 17 h, *Pontus* climbed on a positive horizontal gradient of the chlorophyll signal to locate a high-chlorophyll patch to the northeast.

¹[Online]. Available: <https://coastwatch.pfeg.noaa.gov/erddap/index.html>

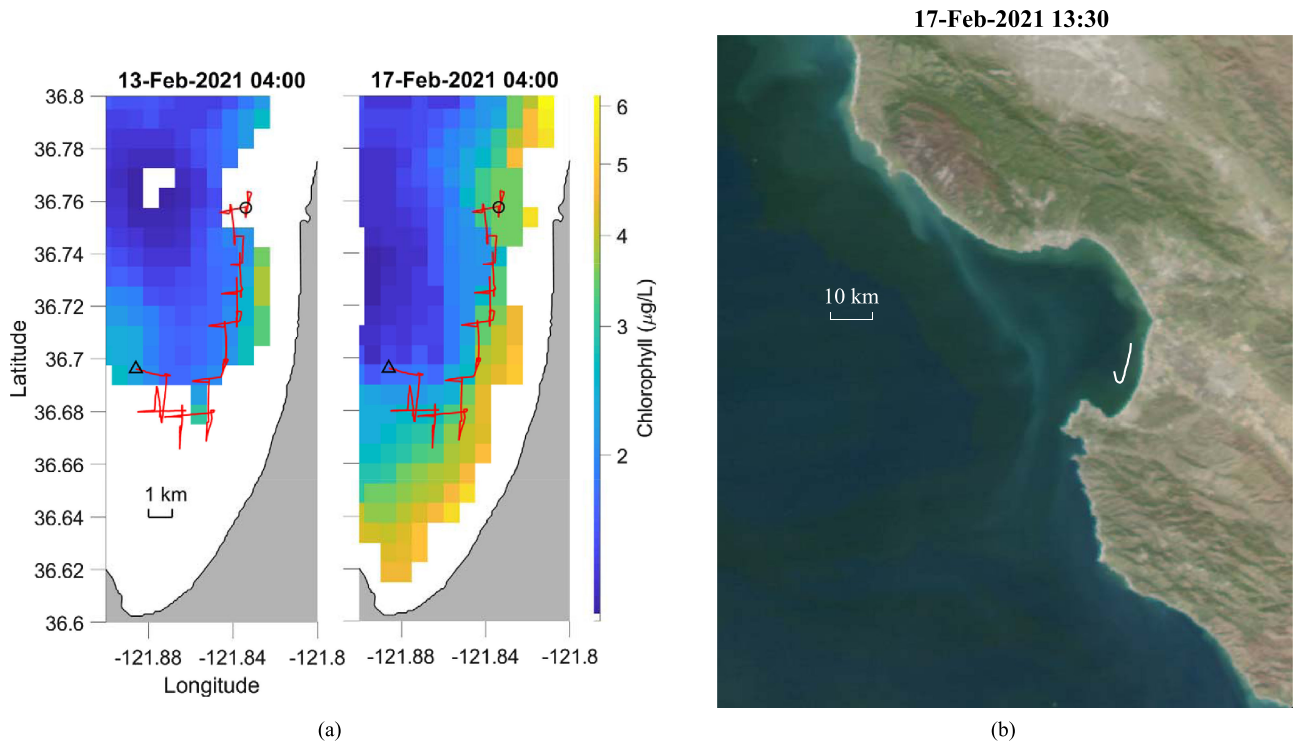


Fig. 4. (a) Satellite-measured sea surface chlorophyll levels in southern Monterey Bay and (b) true-color image of the bay. LRAUV *Pontus*' patch-searching track is overlaid in (a), with the start and end locations marked by the triangle and the circle, respectively. The outline of *Pontus*' track is overlaid in (b) for reference. Time is in Pacific Standard Time.

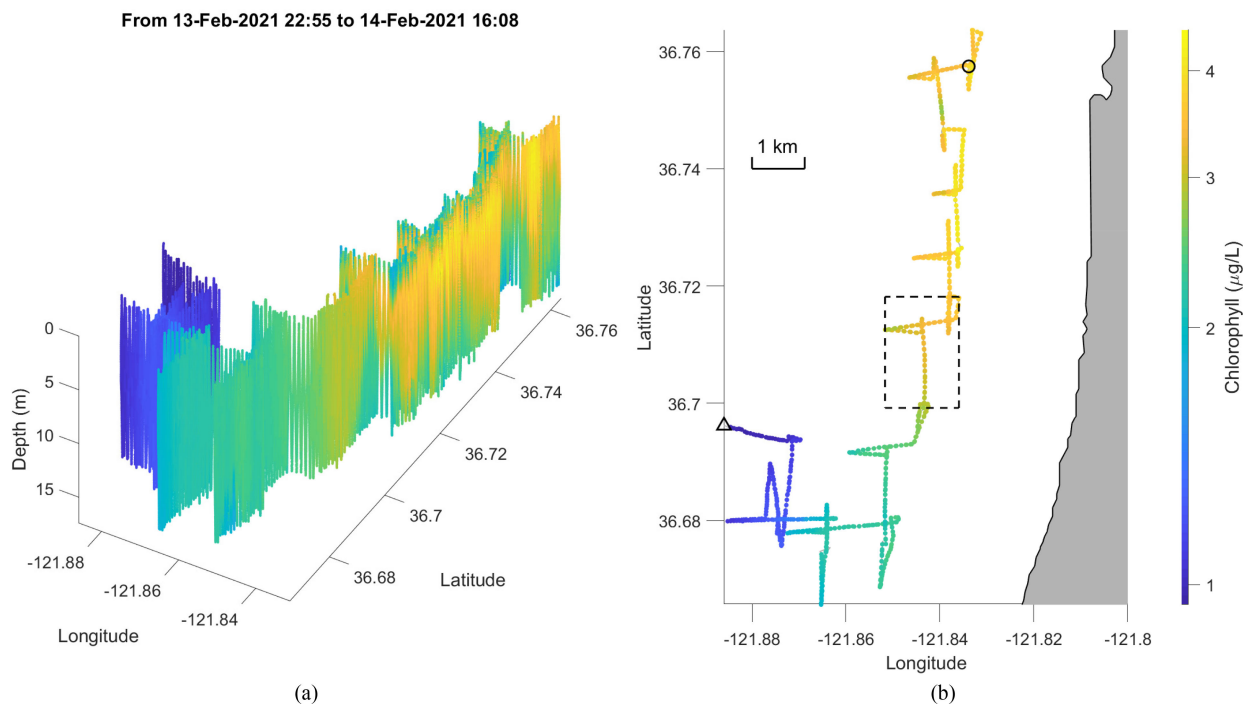


Fig. 5. LRAUV *Pontus* climbed on a positive gradient of chlorophyll to find a patch. (a) Perspective view of chlorophyll on the vehicle track. (b) The chlorophyll peak values on successive yo-yo profiles are color coded. The start and end locations are marked by the triangle and the circle, respectively. One cross-pattern cycle (marked by the dashed box) is shown in Fig. 6. Time is in Pacific Standard Time.

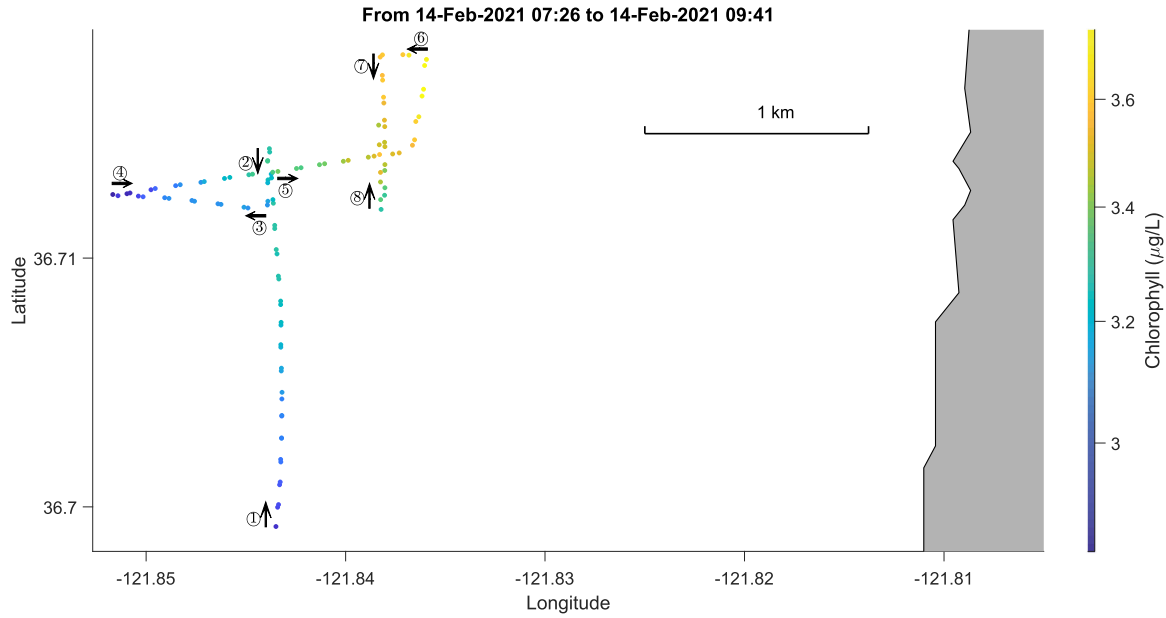


Fig. 6. Close-up view of the cross-pattern cycle marked by the dashed box in Fig. 5. The chlorophyll peak values on successive yo-yo profiles are color coded. Time is in Pacific Standard Time.

In the cross-pattern search, the per-leg distance limit was set to $\text{Dist}_{\text{LegMax}} = 2000$ m, based on the typical scale (a few kilometers) of phytoplankton patches [19], [20]. Prior to the patch tracking mission, LRAUV reconnaissance surveys showed that chlorophyll levels dropped to approximately 90% of chl_{max} at about 2-km distance from the patch center. Hence, we set $\text{Percentage}_{\text{Threshold}} = 90\%$. The per-yoyo chlorophyll peaks were averaged over four yo-yo profiles to smooth out variations. The minimum offshore distance was set to $\text{Dist}_{\text{OffshoreMin}} = 2500$ m to stay away from near-shore shallow bathymetry.

One of the cross-pattern cycles is shown in Fig. 6. Through this cycle, *Pontus* found its way from the low-chlorophyll region to the high-chlorophyll region along a sharp horizontal gradient. The legs are numbered and annotated as follows.

- ① *Northward leg*: The chlorophyll level kept rising until reaching chl_{max} . *Pontus* recorded the chl_{max} value and location. When the vehicle yo-yoed past the chl_{max} location, the chlorophyll level dropped slowly. When the leg distance reached the limit $\text{Dist}_{\text{LegMax}} = 2000$ m (at which point the chlorophyll level was still above $\text{Percentage}_{\text{Threshold}} = 90\%$ of chl_{max}), *Pontus* determined to reverse course and calculated $\text{Dist}_{\text{ToChlMax}}$.
- ② *Southward leg*: *Pontus* traveled $\text{Dist}_{\text{ToChlMax}}$ to return to the chl_{max} location. On this leg, the search-for-maximum function was turned off.
- ③ *Westward leg*: Once returning to the chl_{max} location, *Pontus* made a right turn to yo-yo westward. It turned on the search-for-maximum function and recorded the updated chl_{max} value and location on the path. When the chlorophyll level dropped below $\text{Percentage}_{\text{Threshold}} \cdot \text{chl}_{\text{max}}$, *Pontus* determined to reverse course and calculated $\text{Dist}_{\text{ToChlMax}}$.

- ④ *Eastward leg*: Same as leg 2 except for the direction.
- ⑤ *Continued eastward leg (partly “bent” north-northeastward due to the $\text{Dist}_{\text{OffshoreMin}}$ constraint)*: *Pontus* turned on the search-for-maximum function. When *Pontus* touched the 2.5-km minimum offshore distance limit, it turned to the left onto a course parallel to the coastline so as not to violate the constraint. The chlorophyll level kept rising until reaching chl_{max} . *Pontus* recorded the chl_{max} value and location. When the vehicle yo-yoed past the chl_{max} location, the chlorophyll level dropped slowly. When the leg distance reached $\text{Dist}_{\text{LegMax}}$ (at which point the chlorophyll level was still above $\text{Percentage}_{\text{Threshold}} \cdot \text{chl}_{\text{max}}$), *Pontus* determined to turn to the west (i.e., reverse to the starting eastward direction of this leg) and calculated $\text{Dist}_{\text{ToChlMax}}$.
- ⑥ *Westward leg*: The same as leg 2 except for the direction.
- ⑦ *Southward leg*: The same as leg 3 except that the vehicle made a left turn after returning to the chl_{max} location.
- ⑧ *Northward leg*: The same as leg 2 except for the direction.

Note that in the later portion of leg 5, *Pontus* touched the minimum offshore distance limit. The vehicle turned to north-northeast onto a course parallel to the coastline so as not to violate the constraint. However, the patch-searching behavior, which was running in parallel to the shore avoidance behavior, was not aware of this north-northeastward turn. On the succeeding leg 6, *Pontus* turned westward (reverse to the starting eastward direction of leg 5) “back” to chl_{max} , whereas the actual location of chl_{max} was to the south rather than to the west. This error decreased the accuracy of patch tracking. After the February and April 2021 experiments, we modified the algorithm so that whenever the AUV touches the minimum offshore distance limit, the vehicle reverses course back to chl_{max} detected thus far.

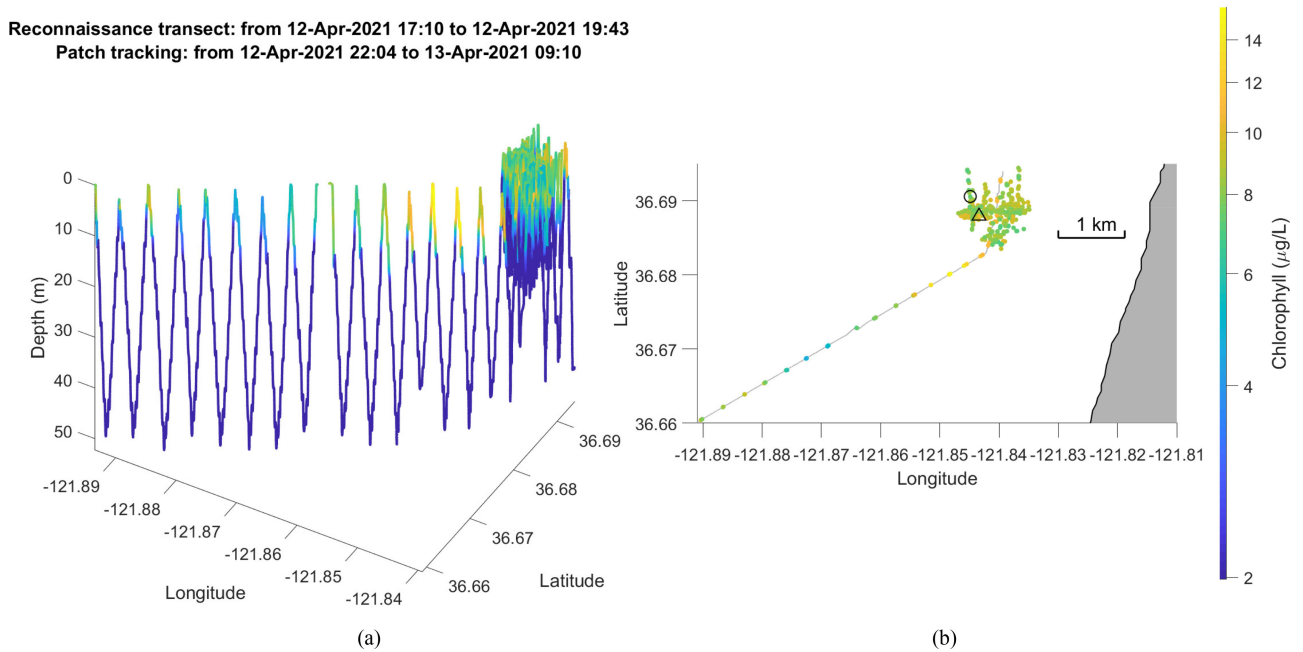


Fig. 7. LRAUV *Pontus* southwest-to-northeast reconnaissance transect and the ensuing patch-tracking segment. (a) Perspective view of chlorophyll levels on the vehicle track. (b) The chlorophyll peak values on successive yo-yo profiles are color coded. The reconnaissance transect is marked by the line track. The start and end locations of the patch-tracking segment are marked by the triangle and the circle, respectively. Time is in Pacific Daylight Time.

If $\text{Percentage}_{\text{Threshold}}$ is set too high or too low, it can cause problems on legs 1, 3, 5, or 7 (see Fig. 2) when the AUV searches for a patch center or probes the boundary of a found patch. If $\text{Percentage}_{\text{Threshold}}$ is set too high, as soon as the chlorophyll level drops only slightly the vehicle will turn back to the “center.” This could get the vehicle trapped in a local chlorophyll maximum, rather than a true center. If $\text{Percentage}_{\text{Threshold}}$ is set too low, it can happen that the vehicle has crossed the patch boundary and has entered a different patch, but the chlorophyll level remains above $\text{Percentage}_{\text{Threshold}} \cdot \text{chl}_{\text{max}}$. This would defeat the purpose of tracking one patch. Statistical analysis on the chlorophyll field data collected in AUV reconnaissance surveys is required for calculating patch scales and specifying appropriate threshold levels to distinguish between true centers and local maxima. These results will inform settings of $\text{Percentage}_{\text{Threshold}}$ and $\text{Dist}_{\text{LegMax}}$. Furthermore, we can improve the algorithm so that $\text{Percentage}_{\text{Threshold}}$ and $\text{Dist}_{\text{LegMax}}$ are adaptively adjusted onboard based on statistics of how much the chlorophyll level drops from chl_{max} when $\text{Dist}_{\text{LegMax}}$ is reached.

B. April 12 and 13, 2021

In another experiment from April 12 to 13, 2021, LRAUV *Pontus* was deployed in southern Monterey Bay to locate and track a phytoplankton patch. *Pontus*’ trajectory and the chlorophyll measurement are shown in Fig. 7, comprising two parts: the reconnaissance transect and the patch-tracking segment. *Pontus* first ran a southwest-to-northeast reconnaissance yo-yo transect from 2- to 50-m depths [see Fig. 7(a)]. During the reconnaissance mission, *Pontus* surfaced every hour for GPS fixes and transmitting decimated data of chlorophyll, temperature, and salinity to shore. When *Pontus* reached a relatively high chlorophyll level

at the northeast end of the reconnaissance transect, the on-shore scientists decided to terminate the reconnaissance mission. After two short tests (not shown), *Pontus* started the patch-tracking segment.

The reconnaissance mission data showed that high chlorophyll levels were in the upper 20 m. Therefore, for patch tracking, we reduced the yo-yo depth range to 1.5–20 m to increase the horizontal resolution. The settings of $\text{Percentage}_{\text{Threshold}}$ and the lengths of the low-pass filters were the same as those used in the February 2021 experiment. Since the reconnaissance mission provided confidence that the start location of patch tracking was at or near a chlorophyll hotspot, we set the maximum distance of each search leg to $\text{Dist}_{\text{LegMax}} = 1000$ m, half that used in the February experiment. The minimum offshore distance was set to $\text{Dist}_{\text{OffshoreMin}} = 1500$ m. Over 11 h, *Pontus* located and tracked a localized patch in an area of about 1 km^2 . The chlorophyll levels in the patch were largely consistent with those measured at the northeast end of the reconnaissance transect, although the elapsed time between the reconnaissance transect and the patch-tracking segment introduced some differences.

VI. CONCLUSION

We developed a method for an AUV to autonomously locate and track phytoplankton patches. A *Tethys*-class LRAUV successfully ran the algorithm in southern Monterey Bay in two experiments. The tracking capability enables observation of phytoplankton communities within a patch while it is moving. In that moving frame of reference, simultaneous observations of environmental conditions capture the processes that drive changes in the phytoplankton community within the patch, similar to a Lagrangian study of microbial

communities in the deep chlorophyll maximum layer in an open-ocean eddy [21]. These methods advance understanding of the factors that cause the growth and decline of marine phytoplankton populations.

While tracking a phytoplankton patch, an AUV can make some of the essential environmental measurements required to understand phytoplankton ecology. Additionally, a *Tethys*-class LRAUV can carry a robotic autonomous molecular analytical instrument to acquire samples and then preserve or process those samples in real time [21], [22]. Such augmentation of onboard sensing is an important technological capability for advancing plankton research. Furthermore, localization and tracking by the AUV can guide additional sampling from ships, for example, when larger amounts of water are needed to fully integrate physical, chemical, and biological sampling. During the April 2021 field experiment, this role of the tracking LRAUV was implemented. Scientists deployed a research vessel with a large water sampling system to the location where the LRAUV had localized a patch. This sampling enabled sufficient water sample acquisition to identify the presence of toxin-producing phytoplankton and the toxin that they produce. Repeated sampling in this manner, in turn, defined the location at which to conduct process studies. Thus, the algorithm demonstrated in this contribution is part of a larger observing strategy, in which autonomous platforms can guide the operations of a much larger fleet. The algorithm can be adapted for locating and tracking other patchy features, such as oil spills.

ACKNOWLEDGMENT

The authors would like to thank Erik Trauschke for helping with the LRAUV operation. The authors appreciate the helpful comments from the anonymous reviewers that improved this paper.

REFERENCES

- [1] C. B. Field, M. J. Behrenfeld, J. T. Randerson, and P. Falkowski, "Primary production of the biosphere: Integrating terrestrial and oceanic components," *Science*, vol. 281, pp. 237–240, 2007.
- [2] M. J. Behrenfeld *et al.*, "Biospheric primary production during an ENSO transition," *Science*, vol. 291, pp. 2594–2597, 2001.
- [3] C. A. Scholin *et al.*, "Mortality of sea lions along the central California coast linked to a toxic diatom bloom," *Nature*, vol. 403, pp. 80–84, Jan. 2000.
- [4] A. P. Martin, "Phytoplankton patchiness: The role of lateral stirring and mixing," *Prog. Oceanogr.*, vol. 57, pp. 125–174, 2003.
- [5] D. J. McGillicuddy, Jr., and P. J. S. Franks, *Models of Plankton Patchiness* (ser. Encyclopedia of Ocean Sciences), J. K. Cochran, H. J. Bokuniewicz, and P. L. Yager, Eds. Amsterdam, The Netherlands: Elsevier, 2019, pp. 536–546.
- [6] G. Johnsen *et al.*, "The advective origin of an under-ice spring bloom in the Arctic Ocean using multiple observational platforms," *Polar Biol.*, vol. 41, pp. 1197–1216, 2018.
- [7] M. Godin, Y. Zhang, J. P. Ryan, T. T. Hoover, and J. G. Bellingham, "Phytoplankton bloom patch center localization by the Tethys autonomous underwater vehicle," in *Proc. MTS/IEEE OCEANS Conf.*, Kona, HI, USA, Sep. 2011, pp. 1–6.
- [8] Y. Zhang *et al.*, "Tracking and sampling of a phytoplankton patch by an autonomous underwater vehicle in drifting mode," in *Proc. MTS/IEEE OCEANS Conf.*, Washington, DC, USA, Oct. 2015, pp. 1–5.
- [9] J. S. Beckler, E. Arutunian, T. Moore, B. Currier, E. Milbrandt, and S. Duncan, "Coastal harmful algae bloom monitoring via a sustainable, sail-powered mobile platform," *Front. Mar. Sci.*, vol. 6, Oct. 2019, Art. no. 587.

- [10] J. A. Farrell, S. Pang, and W. Li, "Chemical plume tracing via an autonomous underwater vehicle," *IEEE J. Ocean. Eng.*, vol. 30, no. 2, pp. 428–442, Apr. 2005.
- [11] A. L. Kukulya *et al.*, "Autonomous chemical plume detection and mapping demonstration results with a COTS AUV and sensor package," in *Proc. MTS/IEEE OCEANS Conf.*, Charleston, SC, USA, Sep. 2018, pp. 1–6.
- [12] E. Burian, D. Yoerger, A. Bradley, and H. Singh, "Gradient search with autonomous underwater vehicles using scalar measurements," in *Proc. IEEE Symp. Auton. Underwater Veh. Technol.*, Monterey, CA, USA, Jun. 1996, pp. 86–98.
- [13] T. O. Fossum *et al.*, "Toward adaptive robotic sampling of phytoplankton in the coastal ocean," *Sci. Robot.*, vol. 4, 2019, Art. no. eaav3041.
- [14] B. Hobson, J. G. Bellingham, B. Kieft, R. McEwen, M. Godin, and Y. Zhang, "Tethys-class long range AUVs—Extending the endurance of propeller-driven cruising AUVs from days to weeks," in *Proc. IEEE/OES Auton. Underwater Veh.*, Southampton, U.K., Sep. 2012, pp. 1–8.
- [15] J. G. Bellingham *et al.*, "Efficient propulsion for the Tethys long-range autonomous underwater vehicle," in *Proc. IEEE/OES Auton. Underwater Veh.*, Monterey, CA, USA, Sep. 2010, pp. 1–6.
- [16] J. G. Bellingham and T. R. Consi, "State configured layered control," in *Proc. IARP 1st Workshop Mobile Robot. Subsea Environ.*, Monterey, CA, USA, Oct. 1990, pp. 75–80.
- [17] M. A. Godin, J. G. Bellingham, B. Kieft, and R. McEwen, "Scripting language for state configured layered control of the Tethys long range autonomous underwater vehicle," in *Proc. MTS/IEEE OCEANS Conf.*, Seattle, WA, USA, Sep. 2010, pp. 1–7.
- [18] Y. Zhang, J. G. Bellingham, M. A. Godin, and J. P. Ryan, "Using an autonomous underwater vehicle to track the thermocline based on peak-gradient detection," *IEEE J. Ocean. Eng.*, vol. 37, no. 3, pp. 544–553, Jul. 2012.
- [19] J. S. Wroblewski, J. J. O'Brien, and T. Platt, "On the physical and biological scales of phytoplankton patchiness in the ocean," *Mémoires Soc. Roy. des Sci. de Liège*, vol. 7, pp. 43–57, 1975.
- [20] M. Scheinin and E. Asmala, "Ubiquitous patchiness in chlorophyll a concentration in coastal archipelago of Baltic Sea," *Front. Mar. Sci.*, vol. 7, Jul. 2020, Art. no. 563.
- [21] Y. Zhang *et al.*, "A system of coordinated autonomous robots for Lagrangian studies of microbes in the oceanic deep chlorophyll maximum," *Sci. Robot.*, vol. 6, 2021, Art. no. eabb9138.
- [22] C. Scholin *et al.*, "The quest to develop ecogenomic sensors: A 25-year history of the Environmental Sample Processor (ESP) as a case study," *Oceanography*, vol. 30, no. 4, pp. 100–113, 2017.



Yanwu Zhang (Senior Member, IEEE) was born in Shaanxi, China, in 1969. He received the B.S. degree in electrical engineering and the M.S. degree in underwater acoustics engineering from Northwestern Polytechnic University, Xi'an, China, in 1989 and 1991, respectively, the M.S. degree in electrical engineering and computer science from the Massachusetts Institute of Technology (MIT), Cambridge, MA, USA, in 1998, and the Ph.D. degree in oceanographic engineering from the MIT/Woods Hole Oceanographic Institution Joint Program, Cambridge/Woods Hole, MA, USA, in 2000.

From 2000 to 2004, he was a Systems Engineer working on medical image processing with the General Electric Company Research and Development Center, Niskayuna, NY, USA, and then a Senior Digital Signal Processing Engineer working on digital communications with Aware Inc., Bedford, MA, USA. Since December 2004, he has been with the Monterey Bay Aquarium Research Institute, Moss Landing, CA, USA, first as a Senior Research Specialist and then as a Senior Research Engineer. He leads the project of targeted sampling by autonomous vehicles, designs adaptive sampling algorithms for marine ecosystem studies, and participated in the development of the Tethys-class long-range autonomous underwater vehicles (LRAUVs). Since 1996, he has participated in more than a dozen field experiments running the Odyssey IIB, Dorado, and Tethys AUVs.

Dr. Zhang was a finalist of the *MIT Technology Review Magazine's* 100 young innovators in 1999. In 2018, he was awarded the Visiting Fellowship of Antarctic Gateway Partnership from University of Tasmania, Hobart, Australia. He was a plenary speaker at the 2020 IEEE OES Autonomous Underwater Vehicle Symposium. He is an Associate Editor for *Frontiers in Marine Science* in the specialty section of Ocean Observation. He is a member of Sigma Xi.



Michael A. Godin was born in Westfield, MA, USA, in 1968. He received the B.S. degree in mechanical engineering from the Worcester Polytechnic Institute, Worcester, MA, in 1991, and the M.S. degree in nuclear engineering from the Massachusetts Institute of Technology, Cambridge, MA, in 1994.

He worked with the U.S. Department of Energy, Washington, DC, USA, from 1991 to 1998, first on robotic handling of spent nuclear fuel and later on program management of nuclear waste cleanup research.

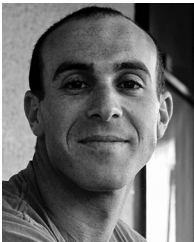
From 1998 to 2003, he worked with Hydro-Optics, Biology, and Instrumentation Labs, Watsonville, CA, USA, on the hardware design, software design, and manufacturing of underwater optical sensors and submersible data loggers. From 2004 to 2012, he was with the Monterey Bay Aquarium Research Institute, Moss Landing, CA, where he developed collaboration systems for geographically distributed groups of researchers, tools for spatio-temporal data exploration, and worked on a new software architecture for implementing state-configured layered control on the Tethys autonomous underwater vehicle (AUV). Since 2013, he has been with IntuAware, Northampton, MA, continuing to support the development of the Tethys AUV. Since 2014, he has worked with CommunicateHealth, Inc., Northampton, developing data-driven and evidence-based web applications for communicating health information.



Brian Kieft received the B.S. degree in computer science from Hope College, Holland, MI, USA, in 2001.

He was with the avionics industry, developing and testing subsystems for military aircraft from 2001 to 2006. In 2006, he joined the Monterey Bay Aquarium Research Institute, Moss Landing, CA, USA, as a Software Engineer. He has worked on various platforms, including mooring controllers, benthic instruments, Wave Gliders, and several autonomous underwater vehicles (AUVs) and their associated payloads.

He has also been actively involved in updating and teaching the IEEE tutorial "AUV Technology and Application Basics" since 2011. He also co-chairs the Wave Glider users group. His current research interests include development of the Tethys-class AUV—a long-range, upper-water-column AUV designed primarily for biological sensing. Apart from development, he also takes part in mission planning and payload integration for ongoing collaborative field programs and engineering tests.



Ben-Yair Raanan received the B.S. degree in marine science from the Ruppin Academic Center, Netanya, Israel, in 2011, and the M.S. degree in marine science (Physical Oceanography Laboratory) from Moss Landing Marine Laboratories, San Jose State University, San Jose, CA, USA, in 2014.

He is currently a Software Engineer with the Monterey Bay Aquarium Research Institute (MBARI), Moss Landing, CA, USA. In 2014, he joined the MBARI as a core developer for MBARI's fleet of autonomous underwater vehicles and works closely

with researchers from a variety of disciplines to develop new enabling technologies for oceanographic research and exploration. His research interests include software design for autonomous robotic systems, machine learning, and artificial intelligence.



John P. Ryan was born in Lafayette, IN, USA, in 1965. He received the B.S. degree in biology from the University of Massachusetts, Boston, MA, USA, in 1988, and the M.S. and Ph.D. degrees in biological oceanography from the University of Rhode Island, Narragansett, RI, USA, in 1993 and 1998, respectively.

In Fall 1998, he joined the Monterey Bay Aquarium Research Institute (MBARI), Moss Landing, CA, USA, as a postdoctoral researcher. He became an MBARI Scientist in 2001 and is currently a Senior

Research Specialist. His research explores relationships between marine life, ranging from microscopic algae to whales, and their environment.

Dr. Ryan received a fellowship from the Office of Naval Research in support of his M.S. research and a NASA New Investigator Research grant in support of his postdoctoral research.



Brett W. Hobson received the B.S. degree in mechanical engineering from San Francisco State University, San Francisco, CA, USA, in 1989.

He began his ocean engineering career with Deep Ocean Engineering, San Leandro, CA, developing remotely operated vehicles. In 1992, he helped start and run Deep Sea Discoveries, where he helped develop and operate deep-towed sonar and camera systems offshore the United States, Venezuela, Spain, and the Philippines. In 1998, he joined Nekton Research, Durham, NC, USA, to design and deploy

bioinspired underwater vehicles for Navy applications. After the merging of Nekton Research into iRobot in 2005, he joined the Monterey Bay Aquarium Research Institute (MBARI), Moss Landing, CA, where he leads the Long-Range Autonomous Underwater Vehicle (LRAUV) program overseeing the development and science operations of six mega-meter-range AUVs. His team has also developed MBARI's long-endurance seafloor crawling Benthic Rover. He teaches AUV tutorials for IEEE/MTS Oceans conferences each year, holds one patent, and is currently Co-Principal Investigator on NASA and National Science Foundation projects aimed at developing novel underwater vehicles for ocean science.